

Virtual element method for semilinear sine-Gordon equation over polygonal mesh using product approximation technique

D Adak^a, S Natarajan^{a,1,*}

^a*Integrated Modelling and Simulation Lab, Department of Mechanical Engineering, Indian Institute of Technology Madras, Chennai-600036, India.*

Abstract

In this paper, we employ the linear virtual element spaces to discretize the semilinear sine-Gordon equation in two dimensions. The salient features of the virtual element method (VEM) are: (a) it does not require explicit form of the shape functions to construct the nonlinear and the bilinear terms, and (b) relaxes the constraint on the mesh topology by allowing the domain to be discretized with general polygons consisting of both convex and concave elements, and (c) easy mesh refinements (hanging nodes and interfaces are allowed). The nonlinear source term is discretized by employing the product approximation technique and for temporal discretization, the Crank-Nicolson scheme is used. The resulting nonlinear equations are solved using the Newton's method. We derive *a priori* error estimations in L^2 and H^1 norms. The convergence properties and the accuracy of the virtual element method for the solution of the sine-Gordon equation are demonstrated with academic numerical experiments.

Keywords: Virtual element method, Product approximation technique, sine-Gordon equation

1. Introduction

The sine-Gordon equation is a nonlinear hyperbolic equation that finds application in a variety of problems in Science and Engineering, viz., shallow-water waves, optical fibers, Josephson-junction, mechanical transmission line, to name a few. The solution of the sine-Gordon equation consists of soliton and multi-soliton solutions. In this direction, several numerical techniques have been employed to study this problem, that includes, finite difference method [1], the finite element method [2], the meshless methods [3] and the boundary element method [4]. Ben-Yu et al. [1] employed the finite difference scheme for the two-dimensional undamped sine-Gordon equation. By exploiting the product approximation techniques, Argyris et al. [2] studied the 2D sine-Gordon equation in the context of the finite element method. Further, Christiansen and Lomdahl [5] employed the generalized leapfrog method to study the solution of the two-dimensional sine-Gordon equation. Aforementioned

*Corresponding author

¹Department of Mechanical Engineering, Indian Institute of Technology Madras, Chennai-600036, India.
E-mail:sundararajan.natarajan@gmail.com; snatarajan@iitm.ac.in

studies focused on undamped sine-Gordon equation. The damped sine-Gordon equation demands more sophisticated numerical techniques. In this direction, the following articles are presented in the literature: Nakajima et al. [6] proposed an efficient numerical technique for the solution of the sine-Gordon equation considering dimensionless loss factors and unit less normalized bias. Recently, a dual reciprocity boundary element method [4] and the radial basis function method [7] have been introduced for the above mentioned model problem. However, most of these techniques require the domain to be discretized with simplex elements such as triangles/quadrilaterals.

The introduction of elements with arbitrary number of sides has revolutionized the simulation technique. Elements with arbitrary number of sides offer greater flexibility in meshing and are less sensitive to mesh distortion [8, 9]. Among the different approaches based on polygonal elements, such as the scaled boundary finite element method [10], the polygonal FEM [8, 11, 12], the strain smoothing techniques [13, 14, 15], the virtual element method (VEM) [16, 17, 18] has an edge. The VEM is a recently developed framework, which provides FEM-like approximations over arbitrary polygonal meshes. Some of the salient features of the VEM are: (a) it does not require an explicit form of the shape functions to compute the bilinear form; (b) it can be applied to convex, and concave elements, i.e., star convexity is not required; (c) easy mesh refinements (hanging nodes and interfaces are allowed) and (d) the degrees of freedom associated with the VEM space, provides sufficient information to compute the discrete bilinear form. Due to its versatility, the method has been applied to a wide variety of problems. Some of them include: the Stokes equation [19], the Plate bending equation [20], linear elliptic, parabolic, and hyperbolic equations [16, 17, 18, 21], linear and nonlinear elasticity problems [22, 23], the convection diffusion equation with small diffusion [24], eigenvalue problems [25, 26], nonconforming VEM for Stokes and elliptic equations [27, 28, 29]. Recently an open source C++ library has been developed by Ortiz-Bernardin et al., [30]. Sutton [31] developed a 50-line MATLAB implementation for the lowest order VEM for the two-dimensional Poisson's problem. Dhanush and Natarajan implemented the VEM into the commercial finite element software Abaqus [32] using user defined subroutines for thermo-elasticity.

However, most of the highlighted works deal with linear model problems. To the best of the authors' knowledge, limited research has been focused on employing the VEM for nonlinear problems. By employing the standard linearization technique, Antonietti et al. [33] introduced the \mathcal{C}^1 VEM for the Cahn-Hilliard problem. Beirão da Veiga et al. designed a new projection operator to approximate the tri-linear term in the Navier-Stokes equation [34]. Recently Adak et al. [35, 36], extended the VEM to semilinear parabolic and hyperbolic equations. The nonlinear term was approximated by employing the L^2 projection operator. However, the difficulty with this approach is that the computation of the Jacobian is numerically expensive, as the Jacobian has to be updated at each time step. To improve the robustness of the VEM, in this paper, we use the product approximation technique [2, 37] to discretize the nonlinear source term in the sine-Gordon equation. The salient feature of the proposed scheme is that it is easy to implement, and it is computable, thus avoiding complicated Jacobian matrix formation.

The rest of the manuscript is organized as follows. In Section 2, we define mesh regularity assumptions for theoretical estimations and the basic notation of Sobolev spaces. In the same section, we introduce the model problem and the weak formulation. In Section 3 we review

the fundamental setting of the virtual element spaces and the corresponding semidiscrete and fully-discrete formulations. In the same section, we define the product approximation techniques for the nonlinear source function in view of the virtual element setting. Error estimations for semi-discrete and fully discrete schemes in respective norms are derived in Section 4. Finally, in Section 5 we investigate the numerical solutions of the sine-Gordon equation with different boundary conditions. A comparison of the proposed approach with the existing technique [35] is discussed in the same section, followed by concluding remarks in the last section.

2. Governing equation and the weak form

Consider the sine-Gordon equation in two space variables

$$D_t^2 u + \gamma D_t u - \Delta u = f(u) \quad (1)$$

in the convex polygonal region $\Omega \subset \mathbb{R}^2$ and $t \in [0, T]$, where γ is the dissipative coefficient and T denotes the final time. The above equation is supplemented with the following boundary conditions:

$$u(x, y, t) = 0 \quad \forall (x, y) \in \partial\Omega; \quad 0 \leq t \leq T, \quad (2)$$

and $f(u) := -\sin u$. Further, the initial conditions are:

$$\begin{aligned} u(x, y, 0) &= h(x, y), \quad \forall (x, y) \in \Omega, \\ D_t u(x, y, 0) &= g(x, y), \quad \forall (x, y) \in \Omega. \end{aligned}$$

The functions $h(x, y)$ and $g(x, y)$ denote the wave modes and their velocity, respectively. Now, multiplying Equation (1) by the test function $v \in H_0^1(\Omega)$ and using Green's theorem, the weak formulation is given by: Given $h(x, y), g(x, y) \in H_0^1(\Omega)$, find $u \in C^0(0, T; H_0^1(\Omega)) \cap C^1(0, T; L^2(\Omega))$ such that [38]:

$$\begin{cases} (D_t^2 u, v) + \gamma (D_t u, v) + a(u, v) = (f(u), v) \quad \forall v \in H_0^1(\Omega), \text{ for a.e. } t \in (0, T], \\ u(0) = h(x, y), \\ D_t u(0) = g(x, y), \end{cases} \quad (3)$$

where

- $D_t^2 u \in L^2(0, T; L^2(\Omega))$ and $D_t u \in L^2(0, T; L^2(\Omega))$ denote the derivatives of u with respect to t .
- (\cdot, \cdot) denotes the global $L^2(\Omega)$ inner product.
- $a(\cdot, \cdot)$ denotes the $H_0^1(\Omega)$ inner-product.

Equation (3) is a second-order nonlinear differential equation with respect to time t , where $f(u)$ is a global Lipschitz continuous function in u and the bilinear form $a(\cdot, \cdot)$ is continuous and coercive, i.e.

$$a(u, v) \leq C \|u\|_{1,\Omega} \|v\|_{1,\Omega} \quad \text{and} \quad a(u, v) \geq \alpha |v|_{1,\Omega} \quad \forall u, v \in H_0^1(\Omega).$$

Hence, problem (3) has a unique solution [39, 40].

3. The virtual element framework

The virtual element method can be seen as a generalization of the finite element method (FEM) that relaxes the constraint on the mesh topology that the FEM otherwise imposes. In this section, we present a brief overview of the VEM.

Notations. Let $\{\mathcal{T}_h\}_h$ be a family of decompositions of Ω into polygonal elements. Let K be an element with diameter h_K and N_K be the total number of vertices of a polygon K . Let us define mesh diameter $h := \max_{K \in \mathcal{T}_h} (h_K)$. For a Banach space H with norm $\|\cdot\|_H$, and a function $\omega : [0, T] \rightarrow H$, that is Lebesgue measurable, the following norms are defined:

$$\|\omega\|_{L^2(0,T;H)} := \left(\int_0^T \|\omega\|_H^2 ds \right)^{1/2} \quad \text{and} \quad \|\omega\|_{L^\infty(0,T;H)} := \operatorname{ess\,sup}_{0 \leq t \leq T} \|\omega(\cdot, t)\|_H.$$

We define

$$L^2(0, T; H) = \{\omega : (0, T] \rightarrow H : \|\omega\|_{L^2(0,T;H)} < \infty\}.$$

The local interpolation approximation properties and the stability of the discrete bilinear forms depend on the mesh regularity, which is stated below [16, 41]. These are later required for estimating the *a priori* estimates in the respective norms (L^2 and H^1 norm).

Assumption 1. (*Mesh regularity*)

- (1) *There exists a real number $\rho > 0$ such that, for all h , each element $K \in \mathcal{T}_h$ is star-shaped with respect to a ball of radius $\geq \rho h_K$.*
- (2) *There exists a constant $c \in (0, 1)$ such that, for all h and for each element $K \in \mathcal{T}_h$, the distance between any two vertices of K is $\geq c h_K$.*

The discrete bilinear forms for the model problem (cf. (1)) are constructed with the help of the following two projection operators (defined element wise),

- The elliptic projection operator $\mathcal{P}_K^\nabla : H^1(K) \rightarrow \mathbb{P}_1(K)$ is defined by:

$$\int_K \nabla(\mathcal{P}_K^\nabla u - u) \cdot \nabla p_1 = 0 \quad \forall p_1 \in \mathbb{P}_1(K) \quad \text{and} \quad P^0(\mathcal{P}_K^\nabla u - u) = 0, \quad (4)$$

$\forall u \in H^1(K)$, where $P^0 u$ is defined as $P^0 u := \frac{1}{|\partial K|} \int_{\partial K} u$.

- The local L^2 projection operator $\mathcal{P}_K^0 : L^2(K) \rightarrow \mathbb{P}_1(K)$, defined by: [28]

$$\left(\mathcal{P}_K^0 q - q, p_1 \right)_{0,K} = 0 \quad \forall p_1 \in \mathbb{P}_1(K), \quad \forall q \in L^2(K). \quad (5)$$

Globally, the projection operator is constructed as $(\mathcal{P}^0 q)|_K = \mathcal{P}_K^0(q)$ for all $q \in L^2(\Omega)$. With these auxiliary space is given by:

$$\mathcal{G}(K) := \left\{ v \in H^1(K) \cap C^0(\partial K) : v|_e \in \mathbb{P}_1(e) \quad \forall e \in \partial K, \quad \Delta v \in \mathbb{P}_1(K) \right\}.$$

We would like to highlight that the elliptic projection operator \mathcal{P}_K^∇ defined in (4) is computable from the vertex values of a function which is in $H^1(K) \cap C^0(\bar{K})$. Hence it is computable for all the function that is in $\mathcal{G}(K)$. Further, using the projection operator \mathcal{P}_K^∇ , we define the local modified VEM space [41]

$$\mathcal{Q}(K) := \left\{ v \in \mathcal{G}(K) : \int_K (\mathcal{P}_K^\nabla v) q = \int_K v q \quad \forall q \in \mathbb{P}_1(K) \right\} \quad K \in \mathcal{T}_h,$$

and the global virtual element space as

$$\mathcal{Q}_h := \left\{ v \in H_0^1(\Omega) : v|_K \in \mathcal{Q}(K) \quad \forall K \in \mathcal{T}_h \right\}.$$

In addition, we would like to highlight that in the modified virtual element space $\mathcal{Q}(K)$, we can compute the projection operator \mathcal{P}_K^0 . The dimension of the local virtual element space $\mathcal{Q}(K)$ is the same as the linear space defined in [16], where the unisolvency is also proved. Further, we define the degrees of freedom (DOFs) associated with $\mathcal{Q}(K)$:

- (\mathbf{d}_1) values of v at the N_K vertexes of K .

The polynomial space $\mathbb{P}_1(K)$ is subset of $\mathcal{Q}(K)$. However, for implementation purpose, we use the set of scaled monomials $\mathcal{M}(K)$ defined in the following manner:

$$\mathcal{M}(K) = \left\{ 1, \frac{x - x_K}{h_K}, \frac{y - y_K}{h_K} \right\}.$$

3.1. Discrete virtual element formulation

Unlike the FEM, the VEM does not require an explicit form of the basis functions η to compute the bilinear forms. By employing the elliptic projection operator \mathcal{P}_K^∇ , we decompose $v_h \in \mathcal{Q}(K)$ as $v_h = \mathcal{P}_K^\nabla(v_h) + (I - \mathcal{P}_K^\nabla)(v_h)$, where $\mathcal{P}_K^\nabla(v_h)$ is the polynomial part and $(I - \mathcal{P}_K^\nabla)(v_h)$ is the nonpolynomial part. The polynomial part can be directly computed using the DOFs, whilst the nonpolynomial part can only be approximated using the DOFs. For each polygon $K \in \mathcal{T}_h$, the discrete bilinear form $a_h^K(\cdot, \cdot) : \mathcal{Q}(K) \times \mathcal{Q}(K) \rightarrow \mathbb{R}$ is defined as follows

$$a_h^K(u_h, v_h) := a^K(\mathcal{P}_K^\nabla(u_h), \mathcal{P}_K^\nabla(v_h)) + S_a^K((I - \mathcal{P}_K^\nabla)u_h, (I - \mathcal{P}_K^\nabla)v_h), \quad (6)$$

where $u_h, v_h \in \mathcal{Q}(K)$ and $S_a^K(\cdot, \cdot)$ is a symmetric bilinear form that ensures stability of the discrete bilinear form $a_h^K(\cdot, \cdot)$. Moreover, the stabilizer $S_a^K(\cdot, \cdot)$ must be spectrally equivalent to the identity matrix and scales as $a^K(\cdot, \cdot)$. The global bilinear form is then given by: $a_h(\cdot, \cdot) : \mathcal{Q}_h \times \mathcal{Q}_h \rightarrow \mathbb{R}$ by adding local contributions as

$$a_h(u_h, v_h) := \sum_{K \in \mathcal{T}_h} a_h^K(u_h, v_h) \quad \forall u_h, v_h \in \mathcal{Q}_h. \quad (7)$$

Following [18, 17] and using the orthogonal L^2 projection operator \mathcal{P}_K^0 , we can formulate the local bilinear form $m_h^K(\cdot, \cdot) : \mathcal{Q}(K) \times \mathcal{Q}(K) \rightarrow \mathbb{R}$ for each polygon K as

$$m_h^K(u_h, v_h) := (\mathcal{P}_K^0 u_h, \mathcal{P}_K^0 v_h) + S_m^K((I - \mathcal{P}_K^0)u_h, (I - \mathcal{P}_K^0)v_h). \quad (8)$$

With the global form given by:

$$m_h(u_h, v_h) = \sum_{K \in \mathcal{T}_h} m_h^K(u_h, v_h) \quad \forall u_h, v_h \in \mathcal{Q}_h. \quad (9)$$

The construction of $a_h^K(\cdot, \cdot)$ and $m_h^K(\cdot, \cdot)$ satisfy the consistency (with respect to polynomials of $\mathbb{P}^1(K)$) and the stability properties. Moreover, we denote the matrix representation of the bilinear forms $a_h(\cdot, \cdot)$ and $m_h(\cdot, \cdot)$ by \mathbf{A} and \mathbf{M} respectively. In particular, $(\mathbf{A})_{ij} = a_h(\eta_i, \eta_j)$ and $(\mathbf{M})_{ij} = m_h(\eta_i, \eta_j)$, where η_i represents the basis function.

Remark 3.1. *In the light of the previous discussion, we highlight that $S_a^K(\cdot, \cdot)$ and $S_m^K(\cdot, \cdot)$ are symmetric bilinear forms on $\mathcal{Q}(K) \times \mathcal{Q}(K)$ that scale like $a^K(\cdot, \cdot)$ and $m^K(\cdot, \cdot)$, respectively. Furthermore, there exist positive constants $\alpha_1, \alpha_2, \beta_1$ and β_2 such that, the following inequalities hold:*

$$\begin{aligned} \alpha_1 a^K(v, v) &\leq S_a^K(v, v) \leq \alpha_2 a^K(v, v) \quad \forall v \in \mathcal{Q}(K) \cap \text{Ker}(\mathcal{P}_K^\nabla) \\ \beta_1 m^K(w, w) &\leq S_m^K(w, w) \leq \beta_2 m^K(w, w) \quad \forall w \in \mathcal{Q}(K) \cap \text{Ker}(\mathcal{P}_K^0), \end{aligned}$$

where $\text{Ker}(\mathcal{P}_K^\nabla)$ and $\text{Ker}(\mathcal{P}_K^0)$ denote the null spaces of \mathcal{P}_K^∇ and \mathcal{P}_K^0 , respectively. There are several choices of the projection operators in the literature [42, 43, 44]. However, we follow the construction provided in [45].

Note that the consistency part of the discrete bilinear forms $a_h(\cdot, \cdot)$ and $m_h(\cdot, \cdot)$ can be directly evaluated using the numerical quadrature. However, in this study, we use the projection operators' matrix representation to evaluate the discrete bilinear form, thus circumventing the numerical quadrature. The projection operators' matrix elements can be assessed using the DOFs [45].

Polynomial-consistency: For all $h > 0$, $\forall K \in \mathcal{T}_h$, the bilinear form $a_h^K(\cdot, \cdot)$ and $m_h^K(\cdot, \cdot)$ satisfies the following consistency property:

$$\begin{aligned} a_h^K(q_1, v_h) &= a^K(q_1, v_h), \\ m_h^K(q_1, v_h) &= (q_1, v_h)_K, \end{aligned} \quad (10)$$

$\forall q_1 \in \mathbb{P}^1(K)$ and $v_h \in \mathcal{Q}(K)$. Further, $a^K(u, v) := \int_K \nabla u \cdot \nabla v$ and $(u, v)_K := \int_K u v$.

Stability: There exist two positive constants α_*, α^* , independent of h and K , such that, for all $v_h \in \mathcal{Q}(K)$, the following condition holds:

$$\begin{aligned} \alpha_* a^K(v_h, v_h) &\leq a_h^K(v_h, v_h) \leq \alpha^* a^K(v_h, v_h) \\ \beta_* m^K(v_h, v_h) &\leq m_h^K(v_h, v_h) \leq \beta^* m^K(v_h, v_h). \end{aligned} \quad (11)$$

The mass matrix associated with the bilinear form $m_h^K(\cdot, \cdot)$ assists to evaluate the nonlinear load term. Furthermore, the interpolation operator $I_h^K : H^2(K) \rightarrow \mathcal{Q}(K)$ and the polynomial approximation $m_\pi \in \mathbb{P}^1(K)$ of a function $m \in H^2(K)$ are introduced for each $K \in \mathcal{T}_h$. We briefly discuss the approximation properties of both the operators. For more details, interested readers are referred to [46, 16].

Lemma 1. For every $h > 0$, $K \in \mathcal{T}_h$, $v \in H^2(K)$, the interpolant $I_h^K v \in \mathcal{Q}(K)$ satisfies

$$\|v - I_h^K v\|_{0,K} + h_K |v - I_h^K v|_{1,K} \leq Ch_K^2 |v|_{2,K}, \quad (12)$$

where C is independent of the local mesh size h_K but depends on the mesh regularity constant ρ .

Proof. See Proposition 4.2 in [25] for more detail. \square

We define the global interpolation operator $I_h : I_h(v_h)|_K := I_h^K(v_h|_K)$. In addition, according to the classical Scott-Dupont principle [17, 47] and exploiting Assumption 1, there is a polynomial approximation in $\mathbb{P}_1(K)$, for all star-shaped polygonal element K that satisfies the following approximation property.

Lemma 2. For every $h > 0$, $K \in \mathcal{T}_h$, $m \in H^2(K)$, there exists a polynomial $m_\pi \in \mathbb{P}_1(K)$ such that

$$\|m - m_\pi\|_{0,K} + h_K |m - m_\pi|_{1,K} \leq Ch_K^2 |m|_{2,K}, \quad (13)$$

where the positive constant C is independent of the mesh size h_K and could be a function of mesh regularity constant ρ .

Proof. See Proposition 4.2 in [16] for more detail. \square

Remark 3.2. The bilinear forms $a_h^K(\cdot, \cdot)$ and $m_h^K(\cdot, \cdot)$ are symmetric positive (semi) definite on $\mathcal{Q}(K) \times \mathcal{Q}(K)$ and can be computed from the DOFs. These bilinear forms consist of a polynomial and a nonpolynomial parts, which reduce to the analogous stiffness and mass matrix of the FEM for polynomial functions. A detailed discussion on the construction of stiffness and mass matrix can be found in [29, 45].

3.2. Construction of the nonlinear source term

In this section, we present a method to discretize the nonlinear load term exploiting the product approximation technique. Making use of analogous ideas as in [2], we approximate the forcing vector (nonlinear load term). Given $\boldsymbol{\eta} = \{\eta_1, \eta_2, \dots, \eta_{N_K}\}$, the local basis functions and $\mathcal{L} := \{l_1, l_2, \dots, l_{N_K}\}$, the DOFs associated with the VEM space $\mathcal{Q}(K)$ over a polygon K , the product approximation for the forcing term is defined as

$$f_h(u_h)|_K := \mathcal{P}_K^0(I_h^K(-\sin(u_h))). \quad (14)$$

Employing approximation (14) and the orthogonality property of \mathcal{P}_K^0 , the load term reduces to the following simple matrix structure:

$$\begin{aligned} F_h(\eta_i) &:= (f_h(u_h), \eta_i) = \int_{\Omega} \mathcal{P}^0 I_h(f(u_h)) \eta_i = \int_{\Omega} I_h(-\sin(u_h)) \mathcal{P}^0 \eta_i \\ &= \sum_{K \in \mathcal{T}_h} \int_K \sum_{j=1}^{N_K} l_j(-\sin(u_h)) \eta_j \mathcal{P}_K^0 \eta_i \\ &= - \sum_{K \in \mathcal{T}_h} \sum_{j=1}^{N_K} \sin(u_h(V_j)) \int_K \mathcal{P}_K^0 \eta_j \mathcal{P}_K^0 \eta_i, \end{aligned} \quad (15)$$

where V_j denotes the j^{th} vertex of a polygon K . Now, by varying the basis function η_i , $1 \leq i \leq N^{\text{dof}}$, we define the discrete forcing vector as:

$$\tilde{f} := \bar{\mathbf{M}} \bar{\mathcal{L}}(-\sin(u_h)), \quad (16)$$

where N^{dof} and $\bar{\mathcal{L}}$ denotes the dimension of the VEM space \mathcal{Q}_h and the global DOFs, respectively and $(\bar{\mathbf{M}})_{ij} = \int_{\Omega} \mathcal{P}^0 \eta_i \mathcal{P}^0 \eta_j$. Further, $\bar{\mathcal{L}}(-\sin(u_h))$ denotes the column vector containing the values of $-\sin(u_h)$ at all the vertices.

Remark 3.3. From the definition of $f_h(u_h)$, it can easily be concluded that the linear functional $F_h(v_h) := (f_h(u_h), v_h)$ is computable from the DOFs associated with the virtual element space \mathcal{Q}_h . Since the DOFs of the linear virtual element space are evaluation of functions at the vertices, $l_j(\sin(u_h)) = \sin(u_h(V_j))$ and therefore the unknowns $u_h(V_j)$ can be computed by standard iteration techniques such as the fixed point iteration technique or Newton's method with a suitable initial guess. However, this formulation may not work for high order virtual element space, since the high order virtual element space ($k \geq 2$) deals with cell moments.

3.3. Discrete scheme

We employ the linear VEM for the discretization of the space variable and the Crank-Nicolson scheme for the temporal variable. Using (7) and (9), the semidiscrete formulation of model problem (3) reads as: find $u_h \in \mathcal{C}^0(0, T; \mathcal{Q}_h) \cap \mathcal{C}^1(0, T; \mathcal{Q}_h)$ such that [48, 21]:

$$\begin{cases} m_h(D_t^2 u_h, v_h) + \gamma m_h(D_t u_h, v_h) + a_h(u_h, v_h) = F_h(v_h) \quad \forall v_h \in \mathcal{Q}_h, \text{ for a.e. } t \in (0, T], \\ u_h(0) = h_0(x, y), \\ D_t u_h(0) = g_0(x, y), \end{cases} \quad (17)$$

where $h_0(x, y)$ and $g_0(x, y)$ denote the interpolant of $h(x, y)$ and $g(x, y)$ on the virtual element space \mathcal{Q}_h . The existence and the uniqueness of the discrete solution u_h follows from the fact that equations (17) are equivalent to a nonlinear initial value problem of second order and $\sin(u)$ is globally Lipschitz continuous in u . Moreover, F_h represents the discrete load term defined in (15). Let $N \in \mathbb{N}$ be a positive integer and consider the time step $\Delta t := T/N$ and for each $t_n = n\Delta t$, we define $u_h^n := u_h(\cdot, t_n)$, where $n = 0, 1, \dots, N$. By employing the θ -weighted scheme for the time discretization and the linear VEM for the spatial discretization, the fully discrete scheme is given by: find $u_h^{n+2} \in \mathcal{Q}_h$ such that

$$\begin{cases} m_h\left(\frac{u_h^{n+2} - 2u_h^{n+1} + u_h^n}{(\Delta t)^2}, v_h\right) + \gamma m_h\left(\frac{u_h^{n+2} - u_h^n}{2\Delta t}, v_h\right) + \theta a_h(u_h^{n+2}, v_h) \\ \quad + (1 - \theta) a_h(u_h^n, v_h) = \left(\theta F_h^{n+2}(v_h) + (1 - \theta) F_h^n(v_h)\right) \quad \forall v_h \in \mathcal{Q}_h, \\ u_h(0) = h_0(x, y), \quad D_t u_h(0) = g_0(x, y). \end{cases} \quad (18)$$

where $F_h^n(v_h) = (f_h(u_h^n), v_h)$. In particular, for $\theta = 1/2$, scheme (18) reduces to the Crank-Nicolson scheme, which is unconditionally stable [49]. Using (16), Equation (18) reduces to, in matrix form:

$$\begin{aligned} & \left[\left(1 + \frac{\gamma \Delta t}{2}\right) \mathbf{M} + (\Delta t^2/2) \mathbf{A} \right] \mathbf{u}^{n+2} + (\Delta t^2/2) \bar{\mathbf{M}} \sin(\mathbf{u}^{n+2}) = 2\mathbf{M} \mathbf{u}^{n+1} \\ & - (\Delta t^2/2) \bar{\mathbf{M}} \sin(\mathbf{u}^n) - \left[\left(1 - \frac{\gamma \Delta t}{2}\right) \mathbf{M} + (\Delta t^2/2) \mathbf{A} \right] \mathbf{u}^n. \end{aligned} \quad (19)$$

Equation (19) represents a system of nonlinear equations and we employ the Newton's method to solve the above system of equations. Since the computation of the matrices, \mathbf{M} , $\bar{\mathbf{M}}$, and \mathbf{A} are done on the VEM space \mathcal{Q}_h using the DOFs, we can readily calculate (19) for any time step t_n . The residual vector is given by:

$$\begin{aligned} \mathcal{R}(\mathbf{u}^{n+2}) := & \left[\left(1 + \frac{\gamma \Delta t}{2}\right) \mathbf{M} + (\Delta t^2/2) \mathbf{A} \right] \mathbf{u}^{n+2} + (\Delta t^2/2) \bar{\mathbf{M}} \sin(\mathbf{u}^{n+2}) \\ & - 2\mathbf{M}\mathbf{u}^{n+1} + (\Delta t^2/2) \bar{\mathbf{M}} \sin(\mathbf{u}^n) + \left[\left(1 - \frac{\gamma \Delta t}{2}\right) \mathbf{M} + (\Delta t^2/2) \mathbf{A} \right] \mathbf{u}^n. \end{aligned} \quad (20)$$

and the Jacobian matrix corresponding to (19) is given by:

$$\mathcal{J}_{ij} := \frac{\partial \mathcal{R}(\mathbf{u}^{n+2})_i}{\partial \mathbf{u}^{n+2}_j} = \left[\left(1 + \frac{\gamma \Delta t}{2}\right) m_{ij} + (\Delta t^2/2) a_{ij} \right] + (\Delta t^2/2) \bar{m}_{ij} \cos(\mathbf{u}^{n+2}_j), \quad (21)$$

where, m_{ij} , a_{ij} and \bar{m}_{ij} are the elements of \mathbf{M} , \mathbf{A} and $\bar{\mathbf{M}}$, respectively. We deduce from (20) and (21) that the residual vector and the Jacobian are numerical integration free and can be considered as readily computable matrix product. By employing the initial condition (3), u^1 is approximated as:

$$\frac{u^1(x, y) - u^0(x, y)}{\Delta t} = I_h(g(x, y)).$$

3.4. Comparison with an existing technique

Here, we briefly recollect the approximation proposed for the load term $F_h(v_h)$ in [35]. Employing the orthogonality property of the local L^2 projection operator \mathcal{P}_K^0 , the nonlinear load term can be computed as

$$\begin{aligned} F_h(v_h) &:= \sum_{K \in \mathcal{T}_h} \int_K f_h(u_h) v_h \\ &= \sum_{K \in \mathcal{T}_h} \int_K -\sin \left(\sum_{i=1}^{N_K} l_i(u_h) \mathcal{P}_K^0 \eta_i \right) \mathcal{P}_K^0 v_h, \end{aligned} \quad (22)$$

where N_K denotes the total number of DOFs of virtual space $\mathcal{Q}(K)$. Thus, if we replace the test function v_h by η_j , we obtain the polynomial representation of the nonlinear load term, which is computable from the information provided by the DOFs associated with the virtual element space $\mathcal{Q}(K)$. Further, the Jacobian matrix corresponding to approximation (22) can be computed as:

$$\begin{aligned} \mathcal{J}_{ij} &= \left[\left(1 + \frac{\gamma \Delta t}{2}\right) m_{ij} + (\Delta t^2/2) a_{ij} \right] \\ &+ (\Delta t^2/2) \sum_{K \in \mathcal{T}_h} \int_K \cos \left(\sum_{j=1}^{N_K} u_j^{n+2} \mathcal{P}_K^0 \eta_j \right) \mathcal{P}_K^0 \eta_j \mathcal{P}_K^0 \eta_i. \end{aligned} \quad (23)$$

It is seen that the above procedure involves integration over the element to compute the Jacobian, moreover, this has to be computed for each time step. Therefore, it can be inferred that the estimation of \mathcal{J}_{ij} is computationally expensive when compared to that of (21).

4. Convergence Analysis:

In this section, we explore *a priori* error estimates for the semi-discrete and the fully discrete system in the L^2 norm and the H^1 seminorm. Since the force function $f(u)$ depends on u , the estimates will depend on the regularity of the discrete solution u_h and $f(u_h)$. In (Lemma 3 in [50], Lemma 2.1 and 2.3 in [51]), the authors proved that $\|u_h\|_{L^2(0,T;H^2(\Omega))} < \infty$ and $\|f(u_h)\|_{L^2(0,T;H^2(\Omega))} < \infty$. However, to emphasize the estimate in terms of regularity of the exact solution u and $f(u)$, we assume that $\|u\|_{L^2(0,T;H^2(\Omega))} < \infty$ and $\|f(u)\|_{L^2(0,T;H^2(\Omega))} < \infty$. In connection with this assumptions, we introduce the elliptic projection operator $P^h : H_0^1(\Omega) \rightarrow \mathcal{Q}_h$, which is defined by

$$a_h(P^h u, v_h) = a(u, v_h) \quad \forall v_h \in \mathcal{Q}_h.$$

Now, we proceed to discuss the approximation properties of P^h , which will be utilized in the convergence analysis. Following Lemma 3.1 in [21], we can derive the results of the following Lemma.

Lemma 3. *Let $u \in H_0^1(\Omega) \cap H^2(\Omega)$ and the domain Ω be convex. Then, there exists a generic constant C independent of the mesh size h such that*

$$\|P^h u - u\|_0 \leq C h^2 |u|_2, \quad |P^h u - u|_1 \leq C h^1 |u|_2. \quad (24)$$

Upon employing the projection operator P^h , we split the term $u - u_h$ as follows:

$$\begin{aligned} u - u_h &= u - P^h u + P^h u - u_h \\ &=: \rho_1 - \rho_2. \end{aligned} \quad (25)$$

The estimation of ρ_1 can be easily done by Lemma 3. To bound the term $\rho_2 (= u_h - P^h u)$, we employ the semi-discrete formulation (17) and the definition of the operator P^h . Note that most of the arguments are adopted from [39] and incorporated in the VEM settings. We explicitly address below the boundedness of the nonlinear load term.

4.1. Optimal L^2 error estimates

Theorem 4.1. *Let $u \in L^2(0,T;H^2(\Omega))$ be the solution of (3) and u_h be the solution of (17), and assume that the $f(u) \in L^2(0,T;H^2(\Omega))$, $D_t u \in L^2(0,T;H^2(\Omega))$, $D_t^2 u \in L^2(0,T;H^2(\Omega))$, $u_0 \in H^2(\Omega)$ and $D_t u(0) \in H^2(\Omega)$. Additionally, let $u_h(0) = I_h(u_0)$ and $D_t u_h(0) = I_h(D_t u(0))$, where I_h is the interpolation operator defined in [45]. Then, $\forall t \in [0,T]$, the following estimate holds :*

$$\begin{aligned} \|(u - u_h)(t)\| &\leq C \left(\|u_{h,0} - u_0\| + \|D_t(u - u_h)(0)\| \right) + C h^2 \left(\|u\|_{L^2(0,T;H^2(\Omega))} \right. \\ &\quad \left. + |u_0|_2 + \|D_t u\|_{L^2(0,T;H^2(\Omega))} + \|D_t^2 u\|_{L^2(0,T;H^2(\Omega))} \right. \\ &\quad \left. + \|f(u)\|_{L^2(0,T;H^2(\Omega))} \right), \end{aligned} \quad (26)$$

where $\|\cdot\|$ denotes $L^2(\Omega)$ norm.

Proof. Using (3) and (17), we can write

$$\begin{aligned}
m_h(D_t^2 \rho_2(t), v_h) + \gamma m_h(D_t \rho_2(t), v_h) + a_h(\rho_2(t), v_h) &= (f_h(u_h) - f(u), v_h) \\
&\quad + (D_t^2 u(t), v_h) - m_h(P^h D_t^2 u(t), v_h) \\
&\quad + \gamma (D_t u(t), v_h) - \gamma m_h(P^h D_t u(t), v_h).
\end{aligned} \tag{27}$$

Since the derivative in the time commutes with $m_h(\cdot, \cdot)$ and (\cdot, \cdot) , Equation (27) can be rewritten as follows:

$$\begin{aligned}
-m_h(D_t \rho_2(t), D_t v_h) + \gamma m_h(D_t \rho_2(t), v_h) + a_h(\rho_2(t), v_h) \\
= D_t m_h(D_t(u - u_h), v_h) + D_t(A_1(t), v_h) \\
- m_h(D_t^2 \rho_1, v_h) - m_h(D_t \rho_1, D_t v_h) - (A_1(t), D_t v_h) \\
+ D_t(A_2(t), v_h) - (A_2(t), D_t v_h) \\
- D_t m_h(A_3(t), v_h) + m_h(A_3(t), D_t v_h) \\
+ \gamma D_t(A_4(t), v_h) - \gamma (A_4(t), D_t v_h) \\
- \gamma D_t m_h(A_5(t), v_h) + \gamma (A_5(t), D_t v_h),
\end{aligned} \tag{28}$$

where $A_1(t), A_2(t), A_3(t), A_4(t)$ and $A_5(t)$ are given by

$$\begin{aligned}
A_1(t) &:= \int_0^t (f_h(u_h) - f(u))(s) ds; \quad A_2(t) := \int_0^t D_t^2 u(s) ds; \\
A_3(t) &:= \int_0^t P^h D_t^2 u(s) ds; \quad A_4(t) := \int_0^t D_t u(s) ds; \\
A_5(t) &:= \int_0^t P^h D_t u(s) ds.
\end{aligned} \tag{29}$$

Define $\hat{\rho}_2(t) := \int_t^\xi \rho_2(s) ds$, where $\xi \in (0, T]$. Upon substituting $v_h = \hat{\rho}_2(t)$ into (28), and noting that $D_t v_h = -\rho_2(t)$, we obtain:

$$\begin{aligned}
m_h(D_t \rho_2(t), \rho_2(t)) + \gamma D_t m_h(\rho_2(t), \hat{\rho}_2(t)) + \gamma m_h(\rho_2(t), \rho_2(t)) + a_h(\rho_2(t), \hat{\rho}_2(t)) \\
= D_t m_h(D_t(u - u_h), \hat{\rho}_2(t)) + D_t(A_1(t), \hat{\rho}_2(t)) \\
- m_h(D_t^2 \rho_1, \hat{\rho}_2(t)) - m_h(D_t \rho_1, D_t \hat{\rho}_2(t)) - (A_1(t), D_t \hat{\rho}_2(t)) \\
+ D_t(A_2(t), \hat{\rho}_2(t)) - (A_2(t), D_t \hat{\rho}_2(t)) \\
- D_t m_h(A_3(t), \hat{\rho}_2(t)) + m_h(A_3(t), D_t \hat{\rho}_2(t)) \\
+ \gamma D_t(A_4(t), \hat{\rho}_2(t)) - \gamma (A_4(t), D_t \hat{\rho}_2(t)) \\
- \gamma D_t m_h(A_5(t), \hat{\rho}_2(t)) + \gamma m_h(A_5(t), D_t \hat{\rho}_2(t)).
\end{aligned} \tag{30}$$

We integrate (30) with respect to t from 0 to ξ and since $a_h(\hat{\rho}_2(0), \hat{\rho}_2(0)) \geq 0$ and $m_h(\rho_2(t), \rho_2(t)) \geq 0$,

we deduce that:

$$\begin{aligned}
\|\rho_2(\xi)\|_h^2 &\leq \|\rho_2(0)\|_h^2 - 2\gamma m_h(\rho_2(0), \hat{\rho}_2(0)) - 2m_h(D_t(u - u_h)(0), \hat{\rho}_2(0)) - 2 \int_0^\xi m_h(D_t^2 \rho_1, \hat{\rho}_2(t)) \\
&\quad + 2 \int_0^\xi m_h(D_t \rho_1, \rho_2(t)) + 2 \int_0^\xi (A_1(t), \rho_2(t)) + 2 \int_0^\xi (A_2(t), \rho_2(t)) \\
&\quad - 2 \int_0^\xi m_h(A_3(t), \rho_2(t)) + 2 \gamma \int_0^\xi (A_4(t), \rho_2(t)) - 2 \gamma \int_0^\xi m_h(A_5(t), \rho_2(t)),
\end{aligned} \tag{31}$$

where $\|\cdot\|_h := m_h(\cdot, \cdot)$ and the integrals in time of terms A_1, A_2, A_3, A_4 and A_5 are transformed through an integration by parts in time. An application of the continuity property of the discrete bilinear form $m_h(\cdot, \cdot)$, Young's inequality, the Cauchy-Schwarz inequality and the approximation property of P^h (Lemma 3), yield the following estimates:

$$|m_h(D_t(u - u_h)(0), \hat{\rho}_2(0))| \leq C \|D_t(u - u_h)(0)\|^2 + C T^2 \int_0^\xi \|\rho_2(t)\|^2 dt, \tag{32}$$

$$\begin{aligned}
\left| \int_0^\xi m_h(D_t^2 \rho_1(t), \hat{\rho}_2(t)) \right| &\leq C \int_0^\xi \|D_t^2 \rho_1(t)\| \|\hat{\rho}_2(t)\| \\
&\leq C h^4 \|D_t^2 u\|_{L^2(0, T; H^2(\Omega))}^2 + C T^2 \int_0^\xi \|\rho_2(t)\|^2 dt,
\end{aligned} \tag{33}$$

and

$$\begin{aligned}
\left| \int_0^\xi m_h(D_t \rho_1, \rho_2(t)) \right| &\leq C \int_0^\xi \|D_t \rho_1\| \|\rho_2(t)\| \\
&\leq C h^4 \|D_t u\|_{L^2(0, T; H^2(\Omega))}^2 + C \int_0^\xi \|\rho_2(t)\|^2 dt.
\end{aligned} \tag{34}$$

Further, we split the load term as follows:

$$\begin{aligned}
f_h(u_h) - f(u) &:= \mathcal{P}^0 I_h(f(u_h)) - f(u) \\
&= \mathcal{P}^0 I_h(f(u_h)) - \mathcal{P}^0 I_h(f(u)) + \mathcal{P}^0 I_h(f(u)) - \mathcal{P}^0 f(u) \\
&\quad + \mathcal{P}^0 f(u) - f(u).
\end{aligned} \tag{35}$$

Since $f(u)$ is a smooth enough, we can write:

$$f(u_h(V_i)) - f(u(V_i)) = f'(\omega_i)(u_h(V_i) - u(V_i)), \tag{36}$$

where, $|f'(\omega_j)| \leq 1$. Therefore, we infer that

$$\begin{aligned}
I_h(f(u_h) - f(u)) &= \sum_{j=1}^{N^{\text{dof}}} f(u_h(V_j)) - f(u(V_j)) \eta_j \\
&= \sum_{j=1}^{N^{\text{dof}}} f'(\omega_i)(u_h(V_i) - u(V_i)) \eta_j \\
&\leq u_h - I_h(u).
\end{aligned} \tag{37}$$

Upon employing the approximation property of I_h and the boundedness of the L^2 orthogonal projection operator \mathcal{P}^0 , we have

$$\begin{aligned} \|\mathcal{P}^0(I_h(f(u_h) - f(u)))\| &\leq \|u_h - I_h(u)\| \\ &\leq \|u_h - u\| + \|u - I_h(u)\| \\ &\leq \|u_h - u\| + C h^2 |u|_2. \end{aligned} \quad (38)$$

Further, since we assume $|f(u)|_2 < \infty$, and using the boundedness of the L^2 orthogonal projection operator and the approximation property of I_h , we obtain

$$\|\mathcal{P}^0 I_h(f(u)) - \mathcal{P}^0 f(u)\| \leq C h^2 |f(u)|_2. \quad (39)$$

and

$$\|\mathcal{P}^0 f(u) - f(u)\| \leq C h^2 |f(u)|_2. \quad (40)$$

An application of Lemma 1 and estimates (38)-(40), yield the bound

$$\|f_h(u_h) - f(u)\| \leq \|u - u_h\| + C h^2 |u|_2 + C h^2 |f(u)|_2. \quad (41)$$

Using analogous technique as in References [36, 39], we obtain:

$$\int_0^\xi (A_1(t), \rho_2(t)) \leq C h^4 \|u\|_{L^2(0,T,H^2(\Omega))}^2 + C h^4 \|f(u)\|_{L^2(0,T,H^2(\Omega))}^2 + C \int_0^\xi \|\rho_2(t)\|^2 dt. \quad (42)$$

Using the polynomial consistency property of $m_h(\cdot, \cdot)$ (c.f. 10) and the result of Lemma 2, we have,

$$\int_0^\xi \left((A_2(t), \rho_2(t)) - m_h(A_3(t), \rho_2(t)) \right) \leq C \left(h^4 \|D_t^2 u\|_{L^2(0,T,H^2(\Omega))}^2 + \int_0^\xi \|\rho_2(t)\|^2 \right), \quad (43)$$

and

$$\int_0^\xi \left((A_4(t), \rho_2(t)) - m_h(A_5(t), \rho_2(t)) \right) \leq C \left(h^4 \|D_t u\|_{L^2(0,T,H^2(\Omega))}^2 + \int_0^\xi \|\rho_2(t)\|^2 \right). \quad (44)$$

substituting inequalities (32)-(34) and (42)-(44) into (31) and using Grownwall's inequality and the stability of $m_h(\cdot, \cdot)$, we obtain:

$$\begin{aligned} \|\rho_2(t)\|^2 &\leq \|\rho_2(0)\|^2 + C \|D_t(u - u_h)(0)\|^2 + C h^4 \left(\|D_t^2 u\|_{L^2(0,T,H^2(\Omega))}^2 \right. \\ &\quad \left. + \|D_t u\|_{L^2(0,T,H^2(\Omega))}^2 + \|u\|_{L^2(0,T,H^2(\Omega))}^2 + \|f(u)\|_{L^2(0,T,H^2(\Omega))}^2 \right). \end{aligned} \quad (45)$$

Upon applying the approximation property of P^h , we write

$$\|\rho_2(0)\|^2 \leq C \left(\|u_h(0) - u_0\|^2 + h^4 |u_0|_2^2 \right), \quad (46)$$

and

$$\|\rho_1(t)\| = \|(u - P^h u)(t)\| \leq C h^2 \left(|u_0|_2 + |D_t u|_{L^1(0,T;H^2(\Omega))} \right). \quad (47)$$

Using (45)-(47), we prove the assertion of the Theorem:

$$\begin{aligned}
& \| (u - u_h)(t) \| \leq \| \rho_1(t) \| + \| \rho_2(t) \| \\
& \leq C \left(\| u_h(0) - u(0) \| + \| D_t(u - u_h)(0) \| \right) + C h^2 \left(|u_0|_2 + \| u \|_{L^2(0,T;H^2(\Omega))} \right. \\
& \quad \left. + \| D_t u \|_{L^2(0,T;H^2(\Omega))} + \| D_t^2 u \|_{L^2(0,T;H^2(\Omega))} + \| f(u) \|_{L^2(0,T;H^2(\Omega))} \right).
\end{aligned}$$

□

Remark 4.1. To derive the first term of the Equation (28) from the Equation (27), we have rewritten Equation (27) into Equation (28) and adjusted with $A_i(t)$. Moreover, we would like to state that in order to derive $\| \rho(t) \|$, we have employed $D_t \hat{\rho}_2(t)$ as the test function. In addition, interested readers are referred to [39] for detail discussion.

4.2. Optimal H^1 error estimates

Theorem 4.2. Let $u \in L^2(0, T; H^2(\Omega))$ be the solution of (3) and u_h be the discrete solution of (17). Moreover, assume that all the assumptions of Theorem (4.1) holds. Then, there exists a positive constant $C(u, f(u))$ independent of the mesh size h , such that the following estimate holds:

$$\begin{aligned}
|u(t) - u_h(t)|_1 & \leq C \left(|u_0 - u_{h,0}|_1 + \| D_t(u - u_h)(0) \| \right) + C h^1 \left(|u_0|_2 \right. \\
& \quad \left. + \| D_t u \|_{L^2(0,T,H^2(\Omega))} \right) + C h^2 \left(|D_t u(0)|_2 + \| u \|_{L^2(0,T,H^2(\Omega))} \right. \\
& \quad \left. + \| D_t^2 u \|_{L^2(0,T,H^2(\Omega))} + \| f(u) \|_{L^2(0,T,H^2(\Omega))} \right) \quad \forall t \in [0, T].
\end{aligned} \tag{48}$$

Proof. The convergence analysis of the error $u - u_h$ in the H^1 norm begins by considering $v_h = D_t \rho_2(t)$ in (27), which follows as:

$$\begin{aligned}
m_h(D_t^2 \rho_2(t), D_t \rho_2(t)) + \gamma m_h(D_t \rho_2(t), D_t \rho_2(t)) + a_h(\rho_2(t), D_t \rho_2(t)) & = (f_h(u_h) - f(u), D_t \rho_2(t)) \\
& + (D_t^2 u(t), D_t \rho_2(t)) - m_h(P^h D_t^2 u(t), D_t \rho_2(t)) \\
& + \gamma (D_t u(t), D_t \rho_2(t)) - \gamma m_h(P^h D_t u(t), D_t \rho_2(t)).
\end{aligned} \tag{49}$$

Since the time derivative commutes with $m_h(\cdot, \cdot)$, and $a_h(\cdot, \cdot)$, and $m_h(D_t \rho_2(t), D_t \rho_2(t)) > 0$, we deduce that:

$$\begin{aligned}
& \frac{1}{2} D_t m_h(D_t \rho_2(t), D_t \rho_2(t)) + \frac{1}{2} D_t a_h(\rho_2(t), \rho_2(t)) \\
& \leq |(f_h(u_h) - f(u), D_t \rho_2(t))| + |(D_t^2 u(t), D_t \rho_2(t)) - m_h(P^h D_t^2 u(t), D_t \rho_2(t))| \\
& \quad + \gamma |(D_t u(t), D_t \rho_2(t)) - m_h(P^h D_t u(t), D_t \rho_2(t))|.
\end{aligned} \tag{50}$$

Using analogous arguments as Theorem 4.3 in [36], we can bound the right hand side terms. An application of similar arguments as (41), we bound the nonlinear load term as

$$|(f_h(u_h) - f(u), D_t \rho_2(t))| \leq C \left(\| u - u_h \|^2 + h^4 |u|_2^2 + h^4 |f(u)|_2^2 \right) + \| D_t \rho_2(t) \|^2. \tag{51}$$

Further, using the polynomial consistency property of $m_h(\cdot, \cdot)$ and Lemma 3, we can write the term as

$$\begin{aligned} |(D_t^2 u(t), D_t \rho_2(t)) - m_h(P^h D_t^2 u(t), D_t \rho_2(t))| &\leq |(D_t^2 u(t), D_t \rho_2(t)) - (\mathcal{P}^0 D_t^2 u(t), D_t \rho_2(t))| \\ &\quad + |(\mathcal{P}^0 D_t^2 u(t), D_t \rho_2(t)) - m_h(P^h D_t^2 u(t), D_t \rho_2(t))| \\ &\leq C h^4 |D_t^2 u(t)|_2^2 + \|D_t \rho_2(t)\|^2. \end{aligned} \quad (52)$$

Similarly, we deduce that

$$|(D_t u(t), D_t \rho_2(t)) - m_h(P^h D_t u(t), D_t \rho_2(t))| \leq C h^4 |D_t u|_2^2 + \|D_t \rho_2(t)\|^2. \quad (53)$$

Upon substituting the estimations (51) - (53) into the Equation (50) and an application of the stability properties of $m_h(\cdot, \cdot)$ and $a_h(\cdot, \cdot)$ (Equation (11)), the Cauchy Schwarz inequality, and integrating (50) from 0 to t , we have

$$\begin{aligned} \|D_t \rho_2(t)\|^2 + |\rho_2(t)|_1^2 &\leq C (\|D_t \rho_2(0)\|^2 + |\rho_2(0)|_1^2) + C h^4 \left(|u_0|_2^2 + \|u\|_{L^2(0,T;H^2(\Omega))}^2 \right. \\ &\quad \left. + \|D_t u\|_{L^2(0,T;H^2(\Omega))}^2 + \|D_t^2 u\|_{L^2(0,T;H^2(\Omega))}^2 + \|f(u)\|_{L^2(0,T;H^2(\Omega))}^2 \right) \\ &\quad + \int_0^t \|D_t \rho_2(s)\|^2 ds. \end{aligned}$$

Utilizing Gronwall's inequality and the estimation $|\rho_1(t)|_1 \leq C h (|u_0|_2 + |D_t u|_{L^1(0,T;H^2(\Omega))})$, we obtain the desired result. \square

Remark 4.2. In the proof of Theorem 4.2, we skipped the proofs of the boundedness of the terms $|(f_h(u_h) - f(u), D_t \rho_2(t))|$, and $|(D_t^2 u(t), D_t \rho_2(t)) - m_h(P^h D_t^2 u(t), D_t \rho_2(t))|$, and $|(D_t u(t), D_t \rho_2(t)) - m_h(P^h D_t u(t), D_t \rho_2(t))|$. These terms can be bounded easily using the polynomial consistency property of $m_h(\cdot, \cdot)$, (10) and the polynomial approximation property (Lemma 2). We refer to Theorem 4.3 in [36] for detailed evidence on the boundedness of the above mentioned terms.

4.3. Error estimation for the fully discrete scheme

Now, we move to derive the error estimations for the fully discrete schemes. To present the analysis unambiguously, we introduce the following notations:

$$\partial_t^2 \rho_2^n := \frac{\rho_2^{n+2} - 2\rho_2^{n+1} + \rho_2^n}{\Delta t^2}; \quad \delta_t \rho_2^n := \frac{\rho_2^{n+2} - \rho_2^n}{2\Delta t}; \quad \rho_{2,1/2}^n := \frac{\rho_2^{n+2} + \rho_2^n}{2}; \quad \partial_t \rho_2 := \frac{\rho_2^1 - \rho_2^0}{\Delta t},$$

where $\rho_2^n := \rho_2(\cdot, t_n)$.

Theorem 4.3. Let u be the analytical solution of (3) and $\{u_h^n\}_n$ be a sequence of discrete solutions satisfying (18) for $\theta = 1/2$. Further, we assume that Assumption 1 holds and $\|\partial_t \rho_2\| + \|\rho_2^1\|_1 + \|\rho_2^0\|_1 = O(h^2 + \Delta t^2)$, $D_t^4 u \in L^2(0, T; L^2(\Omega))$, $D_t^3 u \in L^\infty(0, T; L^2(\Omega))$.

Additionally, let $f(u) \in L^\infty(0, T; H^2(\Omega))$, $D_t u \in L^2(0, T; H^2(\Omega))$, $D_t^2 u \in L^2(0, T; H^2(\Omega))$. Then, there exists a positive constant C such that the following estimation holds:

$$\begin{aligned} \|u(t_n) - u_h^n\| \leq & C \left(\left\| \frac{\rho_2^1 - \rho_2^0}{\Delta t} \right\| + \|\rho_2^1\|_1 + \|\rho_2^0\|_1 \right) \\ & + C (\Delta t)^2 \left(\|D_t^4 u\|_{L^2(0, T; L^2(\Omega))} + \|D_t^3 u\|_{L^\infty(0, T; L^2(\Omega))} \right) \\ & + C h^2 \left(|u(0)|_2 + |D_t u|_{L^2(0, T; H^2(\Omega))} + |D_t^2 u|_{L^2(0, T; H^2(\Omega))} + \|f(u)\|_{L^\infty(0, T; H^2(\Omega))} \right). \end{aligned}$$

Proof. Using the projection operator $P^h u$ at time $t = t_n$, we split the error $u(t_n) - u_h^n := \rho_1^n - \rho_2^n$. Lemma 3 yields the estimation of $\|\rho_1^n\|$. In order to prove the estimation for $\|\rho_2^n\|$, we proceed as follows: Using the equation (18), we can write as

$$\begin{aligned} m_h(\partial_t^2 \rho_2^n, v_h) + \gamma m_h(\delta_t \rho_2^n, v_h) + a_h(\rho_{2,1/2}^n, v_h) &= (f_{h,1/2}^n, v_h) - (f_{1/2}^n, v_h) \\ &\quad - m_h(\partial_t^2 P^h u^n, v_h) + (D_t^2 u_{1/2}^n, v_h) - \gamma m_h(\delta_t P^h u^n, v_h) + \gamma (D_t u_{1/2}^n, v_h). \end{aligned} \quad (54)$$

Adding and subtracting the term $(\partial_t^2 u^n, v_h)$, we have

$$\begin{aligned} m_h(\partial_t^2 P^h u^n, v_h) - (D_t^2 u_{1/2}^n, v_h) &= m_h(\partial_t^2 P^h u^n, v_h) - (\partial_t^2 u^n, v_h) \\ &\quad + (\partial_t^2 u^n, v_h) - (D_t^2 u_{1/2}^n, v_h). \end{aligned}$$

Using analogous arguments as in [52] (Lemma 6), we have

$$|(\partial_t^2 u^n, v_h) - (D_t^2 u_{1/2}^n, v_h)| \leq C \Delta t^3 \|D_t^4 u\|_{L^2(t_{n-1}, t_{n+1}; L^2(\Omega))} \|v_h\|.$$

Further, an application of the polynomial consistency property of $m_h(\cdot, \cdot)$ yields

$$\begin{aligned} |m_h(\partial_t^2 P^h u^n, v_h) - (\partial_t^2 u^n, v_h)| &= |m_h(\partial_t^2 P^h u^n, v_h) - (\mathcal{P}^0(\partial_t^2 u^n), v_h)| \\ &\quad + |(\mathcal{P}^0(\partial_t^2 u^n), v_h) - (\partial_t^2 u^n, v_h)| \\ &\leq C h^2 |\partial_t^2 u^n|_2 \|v_h\|. \end{aligned}$$

Using the polynomial consistency property of $m_h(\cdot, \cdot)$, we have

$$\begin{aligned} | - m_h(\delta_t P^h u^n, v_h) + (\delta_t u^n, v_h) | &= | - m_h(\delta_t P^h u^n, v_h) + (\mathcal{P}^0(\delta_t u^n), v_h) | \\ &\quad | - (\mathcal{P}^0(\delta_t u^n), v_h) + (\delta_t u^n, v_h) | \\ &\leq C h^2 |\delta_t u^n|_2 \|v_h\|. \end{aligned}$$

An application of Taylor's theorem yields

$$| - (\delta_t u^n, v_h) + (D_t u_{1/2}^n, v_h) | \leq C (\Delta t)^2 \|D_t^3 u(t_n)\| \|v_h\|.$$

Further, using the analogous arguments as (41) at time $t = t_n$, we can bound the right hand side as:

$$\|f_h(u_h(t_n)) - f(u(t_n))\| \leq \|u(t_n) - u_h(t_n)\| + C h^2 |u(t_n)|_2 + C h^2 |f(u(t_n))|_2. \quad (55)$$

Substituting $v_h = \frac{\rho_2^{n+2} - \rho_2^n}{2 \Delta t}$ in (54), and exploiting result (55) at time $t = t_n$, we obtain,

$$\begin{aligned}
& \left(\left\| \frac{\rho_2^{n+2} - \rho_2^{n+1}}{\Delta t} \right\|^2 - \left\| \frac{\rho_2^{n+1} - \rho_2^n}{\Delta t} \right\|^2 + \gamma \left\| \frac{\rho_2^{n+2} - \rho_2^n}{2 \Delta t} \right\|^2 + 1/2 (|\rho_2^{n+2}|_1^2 - |\rho_2^n|_1^2) \right) \\
& \leq C (\Delta t)^4 \left(\|D_t^4 u\|_{L^2(t_{n+2}, t_n; L^2(\Omega))}^2 + \|D_t^3 u(t_n)\|^2 \right) + C \Delta t h^4 \left(|u(t_n)|_2^2 + |u(t_{n+2})|_2^2 \right. \\
& \quad \left. + |f(u(t_n))|_2^2 + |f(u(t_{n+2}))|_2^2 + |\partial_t^2 u^n|_2^2 + |\delta_t u^n|_2^2 \right) + \left(\|\rho_2^{n+2}\|^2 + \|\rho_2^n\|^2 \right) \\
& \quad + \left(\left\| \frac{\rho_2^{n+2} - \rho_2^{n+1}}{\Delta t} \right\|^2 + \left\| \frac{\rho_2^{n+1} - \rho_2^n}{\Delta t} \right\|^2 \right). \tag{56}
\end{aligned}$$

Following [52], we can express the term $\partial_t^2 u^n$ as

$$\partial_t^2 u^n = \frac{1}{\Delta t^2} \int_{-\Delta t}^{\Delta t} (\Delta t - |\tau|) D_t^2 u(t_{n+1} + \tau) d\tau.$$

This implies

$$\Delta t \sum_{n=0}^{n-2} |\partial_t^2 u_n|_2^2 \leq \|D_t^2 u\|_{L^2(0, T; H^2(\Omega))}^2.$$

Moreover, we can write the term as

$$\begin{aligned}
& \left(-m_h(\delta_t P^h u^n, v_h) + (D_t u_{1/2}^n, v_h) \right) = \left(-m_h(\delta_t P^h u^n, v_h) + (\delta_t u^n, v_h) \right. \\
& \quad \left. - (\delta_t u^n, v_h) + (D_t u_{1/2}^n, v_h) \right).
\end{aligned}$$

Upon integration, Equation (56) from 0 to $n-2$ and using the discrete Gronwall's inequality, we have

$$\begin{aligned}
\|\rho_2^n\|^2 & \leq C \left(\left\| \frac{\rho_2^1 - \rho_2^0}{\Delta t} \right\|^2 + \|\rho_2^1\|_1^2 + \|\rho_2^0\|_1^2 \right) + C (\Delta t)^4 \left(\|D_t^4 u\|_{L^2(0, T; L^2(\Omega))}^2 \right. \\
& \quad \left. + \|D_t^3 u\|_{L^\infty(0, T; L^2(\Omega))}^2 \right) + C h^4 \left(|u(0)|_2^2 + |D_t u|_{L^2(0, T; H^2(\Omega))}^2 + |D_t^2 u|_{L^2(0, T; H^2(\Omega))}^2 \right. \\
& \quad \left. + \|f(u)\|_{L^\infty(0, T; H^2(\Omega))}^2 \right). \tag{57}
\end{aligned}$$

Using the estimates of ρ_1^n and ρ_2^n , we derive the final result:

$$\begin{aligned}
& \|u(t_n) - u_h^n\| \leq (\|\rho_1^n\| + \|\rho_2^n\|) \\
& \leq C \left(\left\| \frac{\rho_2^1 - \rho_2^0}{\Delta t} \right\| + \|\rho_2^1\|_1 + \|\rho_2^0\|_1 \right) + C (\Delta t)^2 \left(\|D_t^4 u\|_{L^2(0, T; L^2(\Omega))}^2 + \|D_t^3 u\|_{L^\infty(0, T; L^2(\Omega))}^2 \right) \\
& \quad + C h^2 \left(|u(0)|_2 + |D_t u|_{L^2(0, T; H^2(\Omega))} + |D_t^2 u|_{L^2(0, T; H^2(\Omega))} + \|f(u)\|_{L^\infty(0, T; H^2(\Omega))} \right).
\end{aligned}$$

□

5. Numerical Experiments

Four numerical examples are presented in this section to demonstrate the accuracy and the convergence characteristics of the proposed scheme. In all the cases, a rectangular domain is considered and the domain is discretized with different types of meshes, viz., distorted square, non-convex polygons and Voronoi meshes. The random polygonal mesh is generated using Polymesher [53, 29], a polygonal meshing tool based on Matlab. In addition, we also consider concave elements and distorted quadrilateral elements. Figure 1 shows a representative mesh for the distorted square, concave polygons and Voronoi meshes. A pseudocode of the nonlinear solver is given in the Appendix.

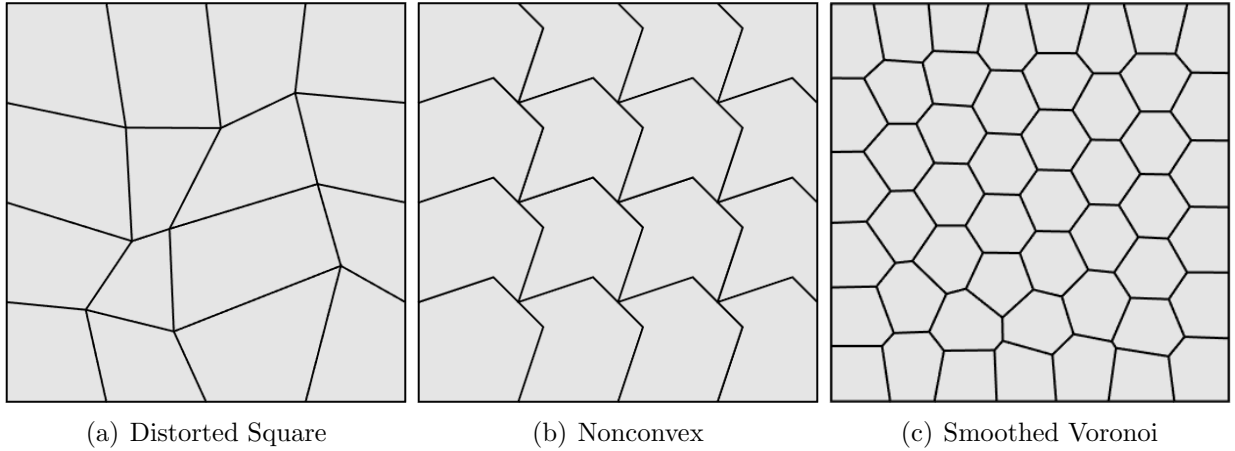


Figure 1: A schematic representation of different discretizations employed in this study.

5.1. Test Problem-1

In the first example, we consider the following two-dimensional sine-Gordon equation

$$\begin{cases} D_t^2 u - \Delta u = f(u) & \text{in } -7 \leq x, y \leq 7 \text{ for } t \in (0, T] \\ u|_{\partial\Omega} = u_0, \end{cases} \quad (58)$$

with the initial conditions:

$$\begin{aligned} u(x, y, 0) &= 4 \tan^{-1}(\exp(x + y)), \quad -7 \leq x, y \leq 7, \\ D_t u(x, y, 0) &= -\frac{4 \exp(x + y)}{1 + \exp(2x + 2y)}, \quad -7 \leq x, y \leq 7. \end{aligned}$$

The analytical solution is given by:

$$u(x, y, t) = 4 \tan^{-1}(\exp(x + y - t)) \quad t \in (0, T]. \quad (59)$$

In Equation (58), u_0 denotes the nonhomogeneous Dirichlet boundary condition that can be determined from the exact solution. The numerical solutions are computed over the nontrivial meshes in the rectangular domain $-7 \leq x, y \leq 7$ at time level $T = 1$. The rate of convergence is evaluated through the relative error in the L^2 norm and the H^1 seminorm,

defined by, which is the difference between the numerical solution u_h and the interpolated solution $I_h u$ at final time T , as:

$$\|I_h u - u_h\|_0^2 := \frac{m_h(I_h u(\cdot, T) - u_h(\cdot, T), I_h u(\cdot, T) - u_h(\cdot, T))}{m_h(I_h u(\cdot, T), I_h u(\cdot, T))} \quad (60)$$

$$|I_h u - u_h|_1^2 := \frac{a_h(I_h u(\cdot, T) - u_h(\cdot, T), I_h u(\cdot, T) - u_h(\cdot, T))}{a_h(I_h u(\cdot, T), I_h u(\cdot, T))}. \quad (61)$$

Figure 2 shows the convergence of the relative error in the L^2 and the H^1 norm with mesh refinement for a variety of meshes including smoothed Voronoi, distorted square and non-convex polygons for two different time steps, $\Delta t = 0.01, 0.5$. For $\Delta t = 0.01$, it can be inferred that the proposed method yields optimal convergence rate of 2 and 1 in L^2 and H^1 , respectively as predicted theoretically in Theorems 4.1 and 4.2 (c.f. Section 4), when the mesh is refined. However, for $\Delta t = 0.05$, the method yields optimal rate of convergence in the H^1 norm, but not in the L^2 norm. This can be attributed to the choice of Δt , which according to the time discretization scheme converges optimally only for sufficiently small Δt .

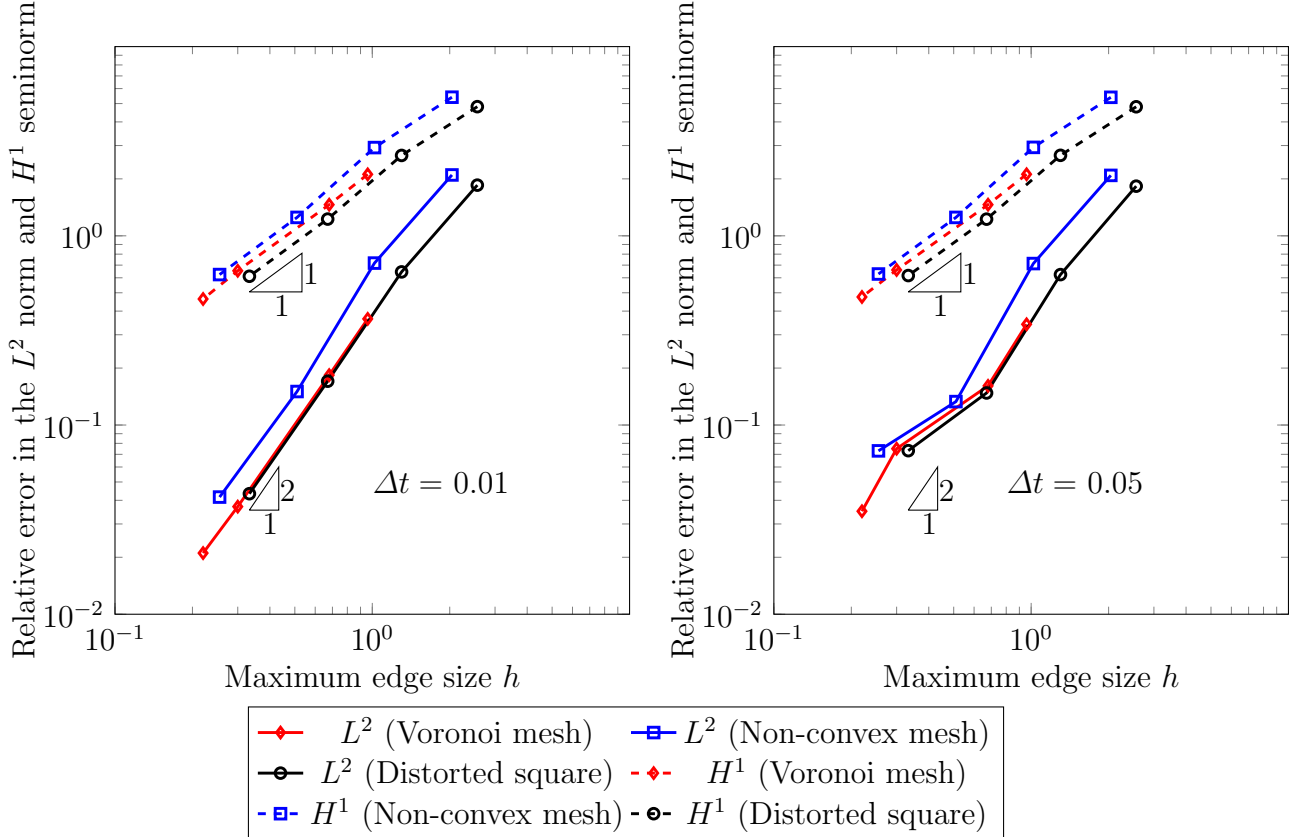


Figure 2: Example 1: convergence of the relative error in the L^2 and H^1 seminorm.

Next, we compare the performance of the proposed approach with that of conventional FE, when the domain is discretized with triangles. Table 1 presents the convergence of the relative error in the L^2 norm and H^1 seminorm. In this case, the domain is discretized with Voronoi meshes and structured triangular elements. The number of elements is kept the same in both the cases. It can be seen that the proposed method and the finite element method yield similar results. The main advantage of using polygonal mesh is that the meshing burden can be alleviated.

Table 1: Convergence of the error in the discrete L^2 norm and the H^1 norm: a comparison between the triangular and polygonal discretizations.

Polygons			Triangles		
DOFs	L^2	H^1	DOFs	L^2	H^1
1002	7.9211×10^{-3}	5.995×10^{-2}	1502	2.1361×10^{-3}	2.4044×10^{-2}
2002	2.6152×10^{-3}	2.4342×10^{-2}	3002	1.0277×10^{-3}	1.1302×10^{-2}
4002	1.0698×10^{-3}	1.2770×10^{-2}	6002	4.8927×10^{-4}	6.9261×10^{-3}
10,002	3.3343×10^{-4}	4.3689×10^{-3}	15,002	2.7891×10^{-4}	3.4745×10^{-3}

5.2. Test Problem-2

Next, we consider the following equation with a nonlinear source term:

$$D_t^2 u - \Delta u = f(u) + g(x, y, t) \text{ on } \Omega \times I, \quad (62)$$

where $\Omega = [0, 1] \times [0, 1]$, and $f(u) = u^2$, and $I = (0, 1]$ with $u = 0$ on $\partial\Omega$. We choose $g(x, y, t)$ such that $u(x, y, t) = e^{-t} x y (1 - x) (1 - y)$ becomes the analytical solution of (62). In this example, we compare the performance of the proposed approach (product approximation technique) to treat the nonlinear term with that of the approach presented in [35]. The domain is discretized with Voronoi meshes and the Crack-Nicolson scheme is employed for the temporal discretization. Table 2 compares the relative error in the L^2 norm, CPU time in seconds and the number of Newton Iterations required between the present approach and the approach presented in [35]. The results are presented for the final time $T = 1$ with a time step, $\Delta t = 0.01$. It is inferred that the present approach requires fewer Newton iterations, which impacts the CPU time required for a similar order of accuracy. Further, we would like to highlight that the convergence analysis is performed for the nonlinear force function $f(u) = -\sin(u)$. Therefore this case ($f(u) = u^2$) is not covered by the theory. However, we have observed that the behaviour of the error is in accordance with that of the sine-Gordon nonlinearity and the error estimations for the case $f(u) = u^2$ can be done with standard modification.

5.3. Test Problem-3

To study the convergence behavior of the fully discrete scheme, consider the problem (62) with $f(u) = -\sin u$ and $g(x, y, t)$ is chosen such that $u(x, y, t) = \sin(t) \sin(\pi x) \sin(\pi y)$ becomes the analytical solution. The results are reported in Table 3. We emphasize that the optimal rate of convergence is observed in temporal direction for very small values of h . The computational domain, the mesh discretization, and final time are considered same as in the Test case 2. The analytical solution is smooth and profoundly depends on the time variable.

Table 2: Convergence of the error in the discrete L^2 norm, CPU time and number of Newton iterations: a comparison between the product approximate technique with the existing technique.

Mesh size	DOFs	Present method			Ref. [35]		
		L^2 Error	CPU-Time (s)	NI	L^2 Error	CPU-time (s)	NI
0.17468	162	3.2820×10^{-3}	0.006974	1	3.2790×10^{-3}	0.118640	4
0.08133	642	7.0280×10^{-4}	0.040384	1	6.9781×10^{-4}	0.533938	4
0.04232	2601	1.5105×10^{-4}	0.381226	2	1.4099×10^{-4}	2.4055	3
0.02088	10601	3.2632×10^{-5}	2.8086	2	3.1079×10^{-5}	11.7883	3

Table 3: Convergence of the relative error in the L^2 norm. The domain is discretized with smoothed Voronoi element.

	Δt	L^2 Error	Rate
$h = .010765$	1/5	4.8610×10^{-4}	-
	1/10	1.4540×10^{-4}	1.74
	1/20	3.6105×10^{-5}	2.00
	1/40	9.1523×10^{-6}	1.98
$h = .014894$	1/5	4.2010×10^{-4}	-
	1/10	1.2403×10^{-4}	1.76
	1/20	3.1441×10^{-5}	1.98
	1/40	7.8060×10^{-6}	2.01

5.4. Collision of four circular solitons

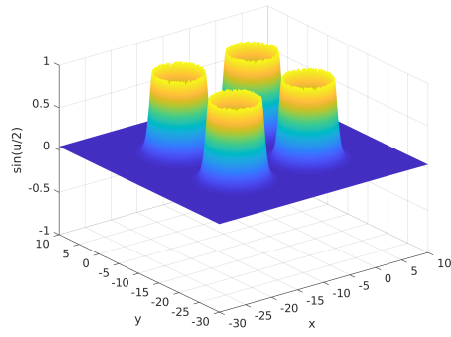
As a last example, we consider the model problem (1) with the dissipative coefficient $\gamma = 0.05$ and the following initial conditions:

$$\begin{aligned}
 h(x, y) &= 4 \tan^{-1}(\exp(\frac{4 - \sqrt{(x+3)^2 + (y+7)^2}}{0.436})), & -10 \leq x \leq 10, & -7 \leq y \leq 7 \\
 g(x, y) &= \frac{4.13}{\cosh(\exp(\frac{4 - \sqrt{(x+3)^2 + (y+7)^2}}{0.436}))}, & -10 \leq x \leq 10, & -7 \leq y \leq 7.
 \end{aligned} \tag{63}$$

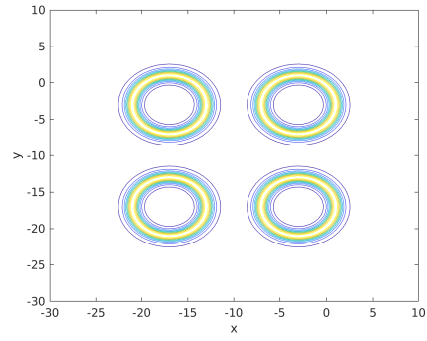
This is a problem of collision of four circular solitons. In this case, we consider homogeneous Neumann boundary condition. We represent the solution over the region $[-10, 30] \times [-10, 30]$ by extending across $x = -10$ and $y = -10$ and exploiting a symmetry relation. The numerical results are depicted in Figure 3 for a mesh size $h \approx 0.45$, the time-step $\Delta t = 0.01$. It is seen that at time $T = 0$, the numerical solution yields four circular rings, which collide with each other and finally (at time $T = 11$) yields one large ring. This is in agreement with the results presented in [7, 2, 54].

6. Conclusion

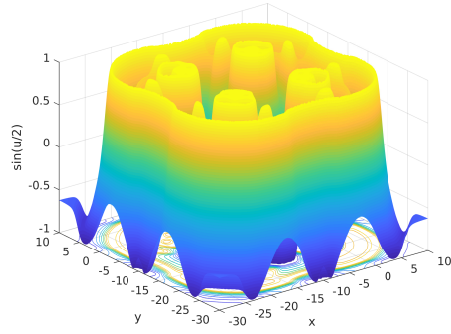
In this paper, we employed the linear VEM to approximate the solutions of the two-dimensional sine-Gordon equation. The nonlinear source term is discretized by employing the product approximation technique. The salient feature of this approach is that the nonlinear



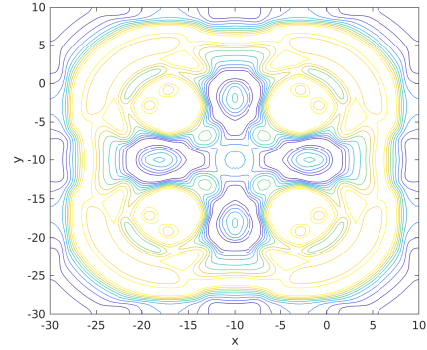
(a) $T = 0$



(b) $T = 0$



(c) $T = 11$



(d) $T = 11$

Figure 3: Collision of four circular ring solitons at time $T = 0$ and $T = 11$.

term is ‘easily’ computable from the DOFs associated with the virtual element space. The proposed scheme offers a very simple Jacobian, which is numerically inexpensive to compute over general polygonal elements. Moreover, VEM is embedded with the advantage of mesh refinements (hanging nodes and interfaces are allowed) which makes computation cheaper. The efficiency and the robustness of the proposed framework are demonstrated with numerical examples with domain discretized with general (possible concave) elements.

7. Extension of the product approximation technique (14) to the high order virtual element space

In Section 3.2, we have discretized the nonlinear load term using the product approximation technique over the linear virtual element space. Within this, we can observe that the product approximation of the nonlinear force function is same as the interpolation of the force function over the virtual element space. Mathematically, this can be expressed as:

$$l_j(\sin(u_h)) = \sin(u_h(V_j)) = \sin(l_j(u_h)), \quad (64)$$

where l_j corresponds to the evaluation of function u_h at the vertex V_j of a polygonal element K . The linear virtual element space deals only with the DOFs at the vertices², which reduces the right hand side of the nonlinear system to a matrix structure, that can be easily evaluated by the mass matrix and the column vector consists of the unknowns (cf Equation (16)).

As the DOFs for the high order virtual element space also includes the cell moments, the above reduction is not feasible. The cell moments are integral of the functions over the polygonal element, K [29]. In (64), if l_j corresponds to the cell moment, i.e. $l_j := \frac{1}{|K|} \int_K m_\alpha u_h$, then we have:

$$l_j(\sin(u_h)) = \frac{1}{|K|} \int_K m_\alpha \sin(u_h), \quad m_\alpha \in \mathcal{M}(K).$$

However, $\sin(l_j(u_h)) = \sin\left(\frac{1}{|K|} \int_K m_\alpha u_h\right)$, which implies $l_j(\sin(u_h)) \neq \sin(l_j(u_h))$. An extension of the product approximation technique to the high order virtual element space, its theoretical estimation and numerical implementation will be a topic for future communications.

²which are evaluation of the functions at the vertices

Appendix

Algorithm 1: Pseudo-code for the implementation of sine-Gordon equation

Compute stiffness matrix \mathbf{A} and mass matrix \mathbf{M}

for $K=1:nele$ **do**

1: Evaluate $\mathbf{A}^K = [a_h^K(\phi_i, \phi_j)]_{N^K \times N^K}$

2: Evaluate $\mathbf{M}^K = [m_h^K(\phi_i, \phi_j)]_{N^K \times N^K}$

3: Evaluate $\bar{\mathbf{M}} = [m_h^K(\mathcal{P}_K^0 \phi_i, \mathcal{P}_K^0 \phi_j)]_{N^K \times N^K}$

4: Assemble local stiffness and mass matrix to form global stiffness and mass matrix.

Solve the nonlinear system of equation using Crank-Nicolson method

1: Create a partition $0 = t_0 < t_1 < \dots < t_m = T$ of the time interval $[0, T]$ with m time-steps $\Delta t = t_l - t_{l-1}$.

2: Set $\mathbf{u}^0 = I_h h(x, y)$

3: Compute \mathbf{u}^1 from initial condition

4: **for** $l=2, \dots, m$ **do**

Solve nonlinear system of equation (18)

$$\begin{aligned} \left[\left(1 + \frac{\gamma \Delta t}{2} \right) \mathbf{M} + (\Delta t^2/2) \mathbf{A} \right] \mathbf{u}^l - (\Delta t^2/2) \tilde{f}^l &= 2 \mathbf{M} \mathbf{u}^{l-1} \\ &+ (\Delta t^2/2) \tilde{f}^{l-1} - \left[\left(1 - \frac{\gamma \Delta t}{2} \right) \mathbf{M} + (\Delta t^2/2) \mathbf{A} \right] \mathbf{u}^{l-2}. \end{aligned}$$

5: Compute error using $I_h u$ and numerical solution \mathbf{u}^m

References

- [1] G. Ben-Yu, P. J. Pascual, M. J. Rodriguez, L. Vázquez, Numerical solution of the sine-Gordon equation, *Appl. Math. Comput.* 18 (1) (1986) 1–14.
- [2] J. Argyris, M. Haase, J. C. Heinrich, Finite element approximation to two-dimensional sine-Gordon solitons, *Comput. Method Appl. M.* 86 (1) (1991) 1–26.
- [3] **Dehghan, Mehdi and Ghesmati, Arezou**, Numerical simulation of two-dimensional sine-Gordon solitons via a local weak meshless technique based on the radial point interpolation method (RPIM), *Comput. Phys.* 181 (4) (2010) 772–786.
- [4] M. Dehghan, D. Mirzaei, The dual reciprocity boundary element method (DRBEM) for two-dimensional sine-Gordon equation, *Comput. Methods Appl. M.* 197 (6-8) (2008) 476–486.
- [5] P. L. Christiansen, P. S. Lomdahl, Numerical study of 2+1 dimensional sine-Gordon solitons, *Physica D.* 2 (3) (1981) 482–494.
- [6] K. Nakajima, Y. Onodera, T. Nakamura, R. Sato, Numerical analysis of vortex motion on Josephson structures, *J. Appl. Phys.* 45 (9) (1974) 4095–4099.
- [7] M. Dehghan, A. Shokri, A numerical method for solution of the two-dimensional sine-Gordon equation using the radial basis functions, *Math. Comput. Simul.* 79 (3) (2008) 700–715.
- [8] N. Sukumar, E. A. Malsch, Recent advances in the construction of polygonal finite element interpolants, *Arch. Comput. Methods Eng.* 13 (1) (2006) 129.
- [9] G. Manzini, A. Russo, N. Sukumar, New perspectives on polygonal and polyhedral finite element method, *Math. Models Methods Appl. Sci.* 24 (2014) 1665–1699.
- [10] S. Natarajan, E. T. Ooi, I. Chiong, C. Song, Convergence and accuracy of displacement based finite element formulation over arbitrary polygons: Laplace interpolants, strain smoothing and scaled boundary polygon formulation, *Finite Elem. Anal. Des.* 85 (2014) 101–122.
- [11] K. Sze, N. Sheng, Polygonal finite element method for nonlinear constitutive modeling of polycrystalline ferroelectrics, *Finite Elem. Anal. Des.* 42 (2) (2005) 107–129.
- [12] J. Bishop, A displacement based finite element formulation for general polyhedra using harmonic shape functions, *Int. J. Numer. Meth. Eng.* 97 (2014) 1–31.
- [13] G. Liu, N. T. Trung, *Smoothed finite element methods*, CRC Press, 2010.
- [14] S. Natarajan, S. P. A. Bordas, E. T. Ooi, Virtual and smoothed finite elements: a connection and its application to polygonal/polyhedral finite element methods, *Int. J. Numer. Meth. Eng.* 104 (2015) 1173–1199.

- [15] A. Francis, A. Ortiz-Bernardin, S. P. A. Bordas, S. Natarajan, Linear smoothed polygonal and polyhedral finite elements, *Int. J. Numer. Meth. Eng.* 109 (9) (2017) 1263–1288.
- [16] L. Beirão da Veiga, F. Brezzi, A. Cangiani, G. Manzini, L. Marini, A. Russo, Basic principles of virtual element methods, *Math. Models Methods Appl. Sci.* 23 (01) (2013) 199–214.
- [17] L. Beirão da Veiga, F. Brezzi, L. Marini, A. Russo, Virtual element method for general second-order elliptic problems on polygonal meshes, *Math. Models Methods Appl. Sci.* 26 (04) (2016) 729–750.
- [18] G. Vacca, L. Beirão da Veiga, Virtual element methods for parabolic problems on polygonal meshes, *Numer. Meth. Partial Differ. Equ.* 31 (6) (2015) 2110–2134.
- [19] P. F. Antonietti, L. B. da Veiga, D. Mora, M. Verani, A stream virtual element formulation of the Stokes problem on polygonal meshes, *SIAM J. Numer. Anal.* 52 (1) (2014) 386–404.
- [20] F. Brezzi, L. D. Marini, Virtual element methods for plate bending problems, *Comput. Methods Appl. Mech. Eng.* 253 (2013) 455–462.
- [21] G. Vacca, Virtual element methods for hyperbolic problems on polygonal meshes, *Comput. Math. Appl.* 74 (2017) 882–898.
- [22] L. Beirão da Veiga, F. Brezzi, L. D. Marini, Virtual elements for linear elasticity problems, *SIAM J. Numer. Anal.* 51 (2) (2013) 794–812.
- [23] L. Beirão da Veiga, C. Lovadina, D. Mora, A virtual element method for elastic and inelastic problems on polytope meshes, *Comput. Methods Appl. Mech. Eng.* 295 (2015) 327–346.
- [24] M. F. Benedetto, S. Berrone, A. Borio, S. Pieraccini, S. Scialò, Order preserving SUPG stabilization for the virtual element formulation of advection-diffusion problems, *Comput. Methods Appl. Mech. Eng.* 311 (2016) 18–40.
- [25] D. Mora, G. Rivera, R. Rodríguez, A virtual element method for the Steklov eigenvalue problem, *Math. Model Methods Appl. Sci.* 25 (08) (2015) 1421–1445.
- [26] O. Čertík, F. Gardini, G. Manzini, G. Vacca, The virtual element method for eigenvalue problems with potential terms on polytopic meshes, *Appl. Math.* 63 (3) (2018) 333–365.
- [27] A. Cangiani, V. Gyrya, G. Manzini, The nonconforming virtual element method for the Stokes equations, *SIAM J. Numer. Anal.* 54 (6) (2016) 3411–3435.
- [28] B. Ayuso de Dios, K. Lipnikov, G. Manzini, The nonconforming virtual element method, *ESAIM: Math. Model. Num* 50 (3) (2016) 879–904.
- [29] A. Cangiani, G. Manzini, O. J. Sutton, Conforming and nonconforming virtual element methods for elliptic problems, *IMA J. Numer. Anal.* 37 (3) (2016) 1317–1354.

- [30] A. Ortiz-Bernardin, C. Alvarez, N. Hitschfeld-Kahler, A. Russo, R. Silva-Valenzuela, E. Olate-Sanzana, Veamy: an extensible object-oriented C++ library for the virtual element method, *Numer. Algorithms* 1–32.
- [31] O. J. Sutton, The virtual element method in 50 lines of matlab, *Numer. Algorithms* 75 (4) (2017) 1141–1159.
- [32] V. Dhanush, S. Natarajan, Implementation of the virtual element method for coupled thermo-elasticity in Abaqus, *Numer. Algorithms* 80 (3) (2019) 1037–1058.
- [33] P. F. Antonietti, L. Beirão da Veiga, S. Scacchi, M. Verani, A C^1 virtual element method for the Cahn-Hilliard equation with polygonal meshes, *SIAM J. Numer. Anal.* 54 (1) (2016) 34–56.
- [34] L. Beirão da Veiga, C. Lovadina, G. Vacca, Virtual elements for the Navier-Stokes problem on polygonal meshes, *SIAM J. Numer. Anal.* 56 (3) (2018) 1210–1242.
- [35] D. Adak, E. Natarajan, S. Kumar, Convergence analysis of virtual element methods for semilinear parabolic problems on polygonal meshes, *Numer. Meth. Part. D. E.* 35 (1) (2019) 222–245.
- [36] D. Adak, E. Natarajan, S. Kumar, Virtual element method for semilinear hyperbolic problems on polygonal meshes, *Int. J. Comput. Math.* 96 (5) (2019) 971–991.
- [37] I. Christie, D. F. Griffiths, A. R. Mitchell, J. M. Sanz-Serna, Product approximation for non-linear problems in the finite element method, *IMA J. Numer. Anal.* 1 (3) (1981) 253–266.
- [38] P. Grisvard, *Singularities in boundary value problems*, Vol. 22, Springer, 1992.
- [39] G. A. Baker, V. A. Dougalis, O. Karakashian, On multistep Galerkin discretizations of semilinear hyperbolic and parabolic equations, *Nonlinear Anal.Theory* 4 (3) (1980) 579–597.
- [40] J. L. Lions, E. Magenes, *Non-homogeneous boundary value problems and applications*, Vol. 1, Springer Science & Business Media, 2012.
- [41] B. Ahmad, A. Alsaedi, F. Brezzi, L. D. Marini, A. Russo, Equivalent projectors for virtual element methods, *Comput. Math. Appl.* 66 (3) (2013) 376–391.
- [42] L. Mascotto, Ill-conditioning in the virtual element method: Stabilizations and bases, *Numer. Meth. Part. D. E.* 34 (4) (2018) 1258–1281.
- [43] L. Beirão da Veiga, F. Dassi, A. Russo, High-order virtual element method on polyhedral meshes, *Comput. Math. Appl.* 74 (5) (2017) 1110–1122.
- [44] F. Dassi, L. Mascotto, Exploring high-order three dimensional virtual elements: bases and stabilizations, *Comput. Math. Appl.* 75 (9) (2018) 3379–3401.

- [45] L. Beirão da Veiga, F. Brezzi, L. Marini, A. Russo, The hitchhiker's guide to the virtual element method, *Math. Models Methods Appl. Sci.* 24 (08) (2014) 1541–1573.
- [46] S. Brenner, R. Scott, The mathematical theory of finite element methods, Vol. 15, Springer Science & Business Media, 2007.
- [47] T. Dupont, R. Scott, Polynomial approximation of functions in sobolev spaces, *Math. Comput.* 34 (150) (1980) 441–463.
- [48] V. Thomée, Galerkin finite element methods for parabolic problems, Vol. 1054, Springer, 1984.
- [49] J. Li, Y.-T. Chen, Computational partial differential equations using MATLAB, Chapman and Hall/CRC Press, 2008.
- [50] S. Larsson, V. Thomée, N.-Y. Zhang, W. Wendland, Interpolation of coefficients and transformation of the dependent variable in finite element methods for the non-linear heat equation, *Math. Method Appl. Sci.* 11 (1) (1989) 105–124.
- [51] C.-M. Chen, S. Larsson, N.-Y. Zhang, Error estimates of optimal order for finite element methods with interpolated coefficients for the nonlinear heat equation, *IMA J. Numer. Anal.* 9 (4) (1989) 507–524.
- [52] T. Dupont, L^2 -estimates for Galerkin methods for second order hyperbolic equations, *SIAM J. Numer. Anal.* 10 (5) (1973) 880–889.
- [53] C. Talischi, G. H. Paulino, A. Pereira, I. F. Menezes, PolyMesher: a general-purpose mesh generator for polygonal elements written in Matlab, *Struct. Multidiscip. O.* 45 (3) (2012) 309–328.
- [54] Q. Sheng, A.-Q. M. Khaliq, D. A. Voss, Numerical simulation of two-dimensional sine-Gordon solitons via a split cosine scheme, *Math. Comput. Simul.* 68 (4) (2005) 355–373.